High-frequency homogenization for layered hyperbolic metamaterials

A. A. Krokhin,[1,*] J. Arriaga,[2] L. N. Gumen,[3] and V. P. Drachev[1,†]

[1]*Department of Physics, University of North Texas, P. O. Box 311427, Denton, Texas 76203-1427*

[2]*Instituto de Física, Universidad Autónoma de Puebla, Apartado Postal J-48, Puebla, 72570, Mexico*

[3]*Universidad Popular Autónoma del Estado de Puebla, 21 Sur, #1103, 72160, Mexico*

(Received 13 October 2015; revised manuscript received 19 January 2016; published 10 February 2016)

We propose an analytical approach for calculation of the homogenized dielectric functions $\epsilon_{\parallel}(\omega)$ and $\epsilon_{\perp}(\omega)$ of one-dimensional periodic metal-dielectric structure. The obtained formulas are valid at high frequencies near the points of topological transition from an elliptic to hyperbolic regime. The proposed method of high-frequency homogenization takes into account rapidly varying electromagnetic fields within the metallic component of a unit cell, in particular, the evanescent character of the plasmonic mode and oscillatory behavior of the waveguidelike modes. Our results show good correspondence to the exact solution of the Rytov's dispersion equation and significant deviation from the widely used quasistatic formulas obtained by spatial averaging along the direction of periodicity z of $\epsilon(z)$ and $1/\epsilon(z)$. The quasistatic approach ignores z dependence of the fields that leads to its limited applicability near the frequency of topological transition.

DOI: 10.1103/PhysRevB.93.075418

I. INTRODUCTION

Uniaxial metamaterials with optical anisotropy going beyond the difference in the absolute values of the components of the dielectric tensor $\epsilon_{ik}(\omega) = \mathrm{diag}(\epsilon_{\parallel},\epsilon_{\parallel},\epsilon_{\perp})$ and showing extreme birefringence when $\epsilon_{\parallel}\,\epsilon_{\perp} < 0$ are known as hyperbolic metamaterials [1–4]. Due to (formally) infinite values of the wave vector allowed by hyperbolic dispersion relation for propagating electromagnetic mode these materials strongly modify the rate and direction of spontaneous emission [5]. The dielectric function of a periodic structure becomes negative at sufficiently low frequencies when the contribution to polarization from the metallic layers overcomes the contribution from the dielectric constituent. Since polarizations along the layers and perpendicular to them differ, the elements of the dielectric tensor $\epsilon_{\parallel}(\omega)$ and $\epsilon_{\perp}(\omega)$ vanish at different frequencies, giving rise to the frequency bands with either elliptic $[\epsilon_{\parallel}(\omega)\,\epsilon_{\perp}(\omega) > 0]$ or hyperbolic $[\epsilon_{\parallel}(\omega)\,\epsilon_{\perp}(\omega) < 0]$ dispersion. Here the subindices $\parallel$ and $\perp$ refer to the propagation parallel or perpendicular to the optical axis, respectively.

The most complete characterization of infinite periodic layered structure is given by Rytov's dispersion equation [6]

$$\cos(K_z d) = \cos(k_{za}a)\cos(k_{zb}b) - \frac{1}{2}\left(\frac{\epsilon_b k_{za}}{\epsilon_a k_{zb}} + \frac{\epsilon_a k_{zb}}{\epsilon_b k_{za}}\right)\sin(k_{za}a)\sin(k_{zb}b), \quad (1)$$

which is an implicit relation between the frequency ω and the Bloch vector $\mathbf{K} = (k_x, k_y, K_z)$ for the transverse-magnetic (TM) eigenmode (vector $\mathbf{H}$ parallel to the layers) propagating at some angle with respect to the optical axis (axis z). Here $k_{za}^2 = \frac{\omega^2}{c^2}\epsilon_a - k^2$ and $k_{zb}^2 = \frac{\omega^2}{c^2}\epsilon_b - k^2$ are the longitudinal components of the wave vector inside the layers a and b, respectively, and $a + b = d$. The system is homogeneous along the xy plane, and therefore the corresponding projection of the transverse wave vector $k = \sqrt{k_x^2 + k_y^2}$ conserves from layer to layer.

For any frequency ω the values of the dielectric functions $\epsilon_{\perp}(\omega)$ and $\epsilon_{||}(\omega)$ can be calculated from the dispersion relation $\omega = \omega(\mathbf{K})$ obtained from Eq. (1). In particular, the well-known quasistatic dielectric constants are easily obtained in the limit $\omega, K \to 0$,

$$\frac{1}{\epsilon_{\perp}} = \frac{f}{\epsilon_a} + \frac{1-f}{\epsilon_b}, \quad (2)$$

$$\epsilon_{||} = \bar{\epsilon} = f\epsilon_a + (1-f)\epsilon_b. \quad (3)$$

Here $f = a/d$ is the portion occupied by material a in a unit cell of length $a + b$.

If the component a of a superlattice (SL) is a metal, then its dielectric function $\epsilon_a(\omega) = 1 - \omega_p^2/\omega^2$ has a pole at $\omega = 0$ that leads to $\epsilon_{||} = -\infty$ and $\epsilon_{\perp} = \epsilon_b/(1-f)$. Because of strong frequency dispersion in metals at low frequencies, calculation of the effective dielectric tensor for hyperbolic materials is not an easy problem. Several homogenization theories have been recently proposed for layered hyperbolic materials. At low (but finite) frequencies Eq. (3) for $\epsilon_{||}$ can be formally rewritten in standard Drude form,

$$\epsilon_{||} = \bar{\epsilon}\left(1 - \frac{\omega_0^2}{\omega^2}\right), \quad (4)$$

with effective plasma frequency

$$\omega_0 = \omega_p\sqrt{\frac{f}{\bar{\epsilon}}} \quad (5)$$

and average permittivity $\bar{\epsilon} = f + (1-f)\epsilon_b$. This formula, obtained in the static limit, ignores the skin effect, and therefore it becomes invalid if the metal layer thickness a becomes comparable with the skin depth $\delta_0 = c/\omega_p$. Strong decay of the electromagnetic field in a thin metal layer and its oscillatory behavior inside a thick dielectric layer allows approximation when the field inside the unit cell is replaced by the field in a

*arkady@unt.edu

†Also at Advanced Materials and Mechanical Processes Institute, University of North Texas, Denton, TX 76203 and with Skolkovo Institute of Science and Technology, Skolkovo, Moscow region, Russia, 143025.

Fabry-Perot resonator. This leads to universal effective plasma frequency [7]

$$\omega_0 = \pi c/(b\sqrt{\epsilon_b}), \tag{6}$$

which is independent of ω_p and metal layer thickness a. This result is in agreement with an idea [8,9] that a metal-dielectric structure with very low metal filling ($f \ll 1$) can be considered a "diluted" metal with effective plasma frequency which depends on geometry of the unit cell but not on metal conductivity. The region of frequencies where a SL exhibits hyperbolic behavior [$\epsilon_{||}(\omega) < 0$] is $0 < \omega < \omega_0$, assuming that within this interval the homogenization conditions $K_z d \ll 1$ is satisfied.

In the region where spatial inhomogeneity of the fields in metal becomes essential ($\delta_0 \leqslant a$), a more advanced approach proposed in Ref. [10] gives the following result:

$$\epsilon_{||}(\omega) = \epsilon_b \left\{ 1 - \frac{1}{1 - \frac{(\omega d/2c)\sqrt{\epsilon_b}}{\tan[(\omega d/2c)\sqrt{\epsilon_b}]} - \frac{\epsilon_b}{f(\epsilon_a(\omega) - \epsilon_b)}} \right\}. \tag{7}$$

It is obtained from earlier developed comprehensive theory of homogenization of bianisotropic periodic medium [11]. Within this approach the result for $\epsilon_\perp$ given by Eq. (2) remains unchanged. Analytically Eq. (7) does not look like the result of the Drude model [Eq. (4)]. However, it is reduced to Eq. (4) in the homogenization limit $d \ll c/\omega$. If the last term in the denominator plays the principal role, i.e., $f \ll (\delta_0/a)^2 \ll 1$, the effective plasma frequency ω_0 is given by Eq. (4). In the opposite case when the skin effect is strongly manifested, $(\delta_0/a)^2 \ll f \ll 1$, the second term in the denominator is expanded up to the quadratic term and the effective plasma frequency can be introduced as follows:

$$\omega_0 = (c/d)\sqrt{12/\epsilon_b}. \tag{8}$$

While numerically this formula is close to the result (6) of Ref. [7], there is a systematic deviation by approximately 10%. The source of this discrepancy is the ratio $\sqrt{12}/\pi \approx 1.103$, which is not exactly 1. This discrepancy is reflected in Fig. 3(a) of Ref. [10], showing that neither Eqs. (4)–(6) nor Eq. (7) give appropriate frequency dependence for the effective permittivity $\epsilon_{||}(\omega)$.

It is important to note that the quasistatic approximation (2) and (3) can be used only within its range of validity and with appropriate justification. While validity of this approximation for metal-dielectric composites long has been criticized [12], it is still widely used. This approximation becomes invalid if the angle of incidence is close to the angle of total internal reflection [13]. Breakdown of the quasistatic approach for this special case has been recently demonstrated experimentally for all-dielectric SL [14]. Applicability of the quasistatic approximation for calculation of the rate of spontaneous emission was analyzed in Refs. [15,16]. It was shown that this approximation usually overestimates the rate. At the same time, the quasistatic approximation may be successfully applied, provided that rigorous justification and range of validity are given [17].

Apart from frequency dispersion a layered (or wired) medium exhibits spatial dispersion which gives rise to k dependence of the effective permittivity [3,4,9,18–21]. Comparison of the exact dispersion relation (1) with the equation of crystal optics in an uniaxial crystal shows that the effective dielectric tensor enquires off-diagonal elements if the wave propagates under some angle to the optical axis [19]. However, these off-diagonal elements vanish for propagation parallel and perpendicular to the optical axis. In the diagonal elements the nonlocal terms appear as k-dependent corrections to the quasistatic values (2) and (3). Here we show that in general case the quasistatic approximation is not valid since the skin effect in metal cannot be neglected at finite frequencies. Therefore, Eqs. (2) and (3) can be used as zero approximation in very limited situations as well as the nonlocal corrections to these quasistatic values. This conclusion is in agreement with the well-known fact that at room temperatures under the conditions of normal skin-effect temporal dispersion in metals is much more important than spatial dispersion [22]. Domination of temporal dispersion also follows from identity of the wave equation in layered hyperbolic metamaterial to the Klein-Gordon equation for a massless field [23].

In order to clarify the problem of frequency dependence of the tensor of effective permittivity of a layered hyperbolic material, we propose a simple homogenization scheme which takes into account the effects of frequency and spatial dispersion directly from Rytov's equation (1). We calculate analytically the effective dielectric functions $\epsilon_{||}(\omega)$ and $\epsilon_\perp(\omega)$ and establish the limits of applicability of the Drude model with effective plasma frequencies (5) and (6) and of the result given by Eq. (7). Propagation in plane of periodicity and parallel to the layers are considered separately. In the latter case the bands originated from the evanescent surface plasmonlike mode and from the oscillating waveguidelike mode lead to different results for the effective dielectric function. The proposed method of homogenization is quite general. It is valid not only for one-dimensional (1D) SL but for any periodic structure. Unlike the quasistatic approach (2) and (3), our method accounts for spatial variation of the fields within the unit cell and, thus, may be valid at high frequencies. For elastic periodic medium a homogenization theory valid at high frequencies was proposed in Ref. [24]. It gives the parameters of the effective medium for the parts of the dispersion curve close to the edge of the Brillouin zone where group velocity vanishes and each Bloch eigenmode becomes a standing wave with the maximum value of the Bloch vector. The term "'high-frequency homogenization" is borrowed from Ref. [24]. Here we are interested in the long-wavelength part of the spectrum, where the Bloch vector is small but the frequency can be arbitrarily high, i.e., our approach is valid close to the center of the Brillouin zone (Γ point). Note that small value of the Bloch vector does not exclude spatial oscillations of the fields in the metallic component of the SL.

II. HOMOGENIZATION OF PERIODIC DISPERSIVE MEDIUM

Homogenization procedures for static fields are well developed for 2D and 3D periodic structures [25–31]. At finite frequencies local resonances as well as the effects of dispersion may lead to strong gradients in the distribution of electric (or magnetic) field within a unit cell. Homogenization procedure in this case requires more sophisticated methods.

Current progress in fabrication and application of optical metamaterials gave rise to more advanced approaches to the problem of calculation of effective medium parameters, see, e.g., Refs. [9,11,32–39]. As a rule calculations of the effective parameters based on these advanced approaches require extensive numerical efforts, which not always can be justified for 1D periodic superlattices. Here we propose relatively simple new analytical method of calculation of $\epsilon_{||}(\omega)$ and $\epsilon_{\perp}(\omega)$. It is based on well-known formulas for phase and group velocities:

$$V_{\rm ph} = \frac{\omega}{k} = \frac{c}{n}, \tag{9}$$

$$V_g = \frac{d\omega}{dk} = \frac{c}{n(\omega) + \omega\frac{dn(\omega)}{d\omega}}. \tag{10}$$

Combining these formulas, a simple differential equation for the effective dielectric function $\epsilon_{\rm eff} = n^2(\omega)$ can be obtained:

$$\frac{c^2}{V_{\rm ph}V_g} = n\left(n + \omega\frac{dn}{d\omega}\right) = \epsilon_{\rm eff} + \frac{1}{2}\omega\frac{d\epsilon_{\rm eff}}{d\omega} = F(\omega). \tag{11}$$

Solution of this equation gives a frequency-dependent dielectric function of the equivalent homogeneous medium

$$\epsilon_{\rm eff}(\omega) = \frac{2}{\omega^2}\int_{\omega_n}^{\omega} \omega' F(\omega')d\omega'. \tag{12}$$

Here ω_n is the constant of integration, which is the frequency where the effective dielectric function vanishes, i.e., $\epsilon_{\rm eff}(\omega_n)$=0. Thus, Eq. (12) defines *exactly* the effective dielectric function if the group and the phase velocities are known within some interval of frequencies. In what follows we calculate the function $F(\omega)$ for metal-dielectric SL, obtain two dielectric functions $\epsilon_{||}(\omega)$ and $\epsilon_{\perp}(\omega)$, and apply these results for different metal-dielectric SL.

III. PROPAGATION PERPENDICULAR TO THE LAYERS

For the wave propagating along axis z the Bloch vector $\mathbf{K} = (0,0,K)$ and $k_x = k_y = 0$. The component a of the superlattice is a metal with $\epsilon_a = -|\epsilon(\omega)|$ and the component b is a dielectric. The local wave vector in metal is $k_{za} = i(\omega/c)\sqrt{|\epsilon(\omega)|} = i/\delta$, where $\delta(\omega) = c/(\omega\sqrt{|\epsilon(\omega)|})$ is the skin depth. In the limit of frequencies well below ω_p the skin depth approaches its lowest limiting value $\delta_0 = c/\omega_p$. Taking into account that k_{za} is pure imaginary, the dispersion equation (1) is rewritten in the following form:

$$D_{||}(\omega) = \cos(Kd), \tag{13}$$

where

$$D_{||}(\omega) = \cosh\left[\frac{a}{\delta(\omega)}\right]\cos\left(\frac{\omega b}{c}\sqrt{\epsilon_b}\right) + \frac{1}{2}\left[\sqrt{\frac{|\epsilon(\omega)|}{\epsilon_b}} - \sqrt{\frac{\epsilon_b}{|\epsilon(\omega)|}}\right]\sinh\left[\frac{a}{\delta(\omega)}\right]\sin\left(\frac{\omega b}{c}\sqrt{\epsilon_b}\right). \tag{14}$$

Calculating the derivative $d\omega/dK$ and the ratio ω/K from Eq. (13) we obtain

$$F(\omega) = c^2\frac{K}{\omega}\frac{dK}{d\omega} = -\frac{c^2}{d^2}\frac{Kd}{\sin(Kd)}\frac{1}{\omega}\frac{dD(\omega)}{d\omega}. \tag{15}$$

In the homogenization limit $Kd \ll 1$ the ratio $Kd/\sin(Kd)$ can be replaced by 1. Substitution of Eq. (15) into Eq. (12) gives the final result for the effective dielectric function:

$$\epsilon_{||}(\omega) \approx \frac{2c^2}{\omega^2 d^2}[D_{||}(\omega_n) - D_{||}(\omega)] = \frac{2c^2}{\omega^2 d^2}[1 - D_{||}(\omega)]. \tag{16}$$

Here we used that $D_{||}(\omega_n) = 1$. This property originates from Eq. (12) where ω_n is defined as a frequency separating the region of transparency ($\epsilon_{\rm eff} > 0$) from the region where propagation is prohibited ($\epsilon_{\rm eff} < 0$). Spectrum of metal-dielectric SL has a gap which starts at $\omega = 0$. The gap appears because $D_{||}(\omega = 0) = \cosh(a/\delta_0) + (b/2\delta_0)\sinh(a/\delta_0) > 1$, i.e., the dispersion equation (13) does not have real solution for K. However, the function $D_{||}(\omega)$ decreases and oscillates with ω. A series of frequencies ω_n, giving rise to a series of allowed zones starting at $K = 0$ are obtained from the equation

$$D_{||}(\omega_n) = 1. \tag{17}$$

This equation has an infinite number of solutions, $\omega_1 < \omega_2 < \omega_3 < \cdots$.

For frequencies higher than ω_n the SL is transparent, i.e., each ω_n plays the role of the effective plasma frequency. Spectrum of metal-dielectric SL has an infinite number of allowed bands separated by gaps. Thus, it is a metamaterial which exhibits plasmalike behavior within several intervals of frequencies. Each frequency ω_n is a point of an optical topological transition [40]. The lowest frequency ω_1 is the most interesting point of transition since the gap below it and the allowed zone above it are usually the widest in the spectrum of the SL.

Note that unlike the formulas (5), (6), and (8), which are valid within some approximations, the solutions of Eq. (17) give the exact values for the effective plasma frequency. The effective plasma frequency ω_n depends in general on the properties of the metal and the dielectric and on the geometry of the unit cell. In the case of small filling fractions, $f \ll 1$, the effective plasma frequency ω_1 lies well below ω_p. At these frequencies $|\epsilon(\omega_1)| \gg \epsilon_b$ and the second term in Eq. (14) gives the principal contribution. The solutions of Eq. (17) are close to the solutions of the equation $\sin(\omega b\sqrt{\epsilon_b}/c) = 0$, i.e., the lowest solution ω_1 is close to ω_0 given by Eq. (6). In previous studies [7,41] one more condition, $\delta_0 \sim a$, is usually required for the effective plasma frequency to be given by Eq. (6). However, it is easy to see that even if $a \gg \delta_0$ the effective plasma frequency ω_1 still can be approximated by Eq. (6), provided that $\omega_0 \ll \omega_p$.

The quasistatic result (5) is obtained from Eq. (17) in the low-frequency limit $(\omega b/c)\sqrt{\epsilon_b} \ll 1$ when the skin effect is negligible, $a \ll \delta(\omega)$. While the result given by Eq. (8) cannot be obtained from the exact equation $D(\omega_i) = 1$, numerically ω_0 becomes close to ω_1 in the limit of small filling, $f \ll 1$.

The formula (16) for the effective dielectric function is valid not only within the first gap and first transmission band but also for *any* frequency in the vicinity of the Γ point. It is also valid not only for a metal-dielectric SL but for a SL of any constituents if $D(\omega)$ is replaced by the right-hand side of Rytov's equation (1). The only approximation used in derivation of the effective dielectric function is $Kd/\sin(Kd) = 1 + O(K^2d^2)$, i.e., Eq. (16) is valid in a linear

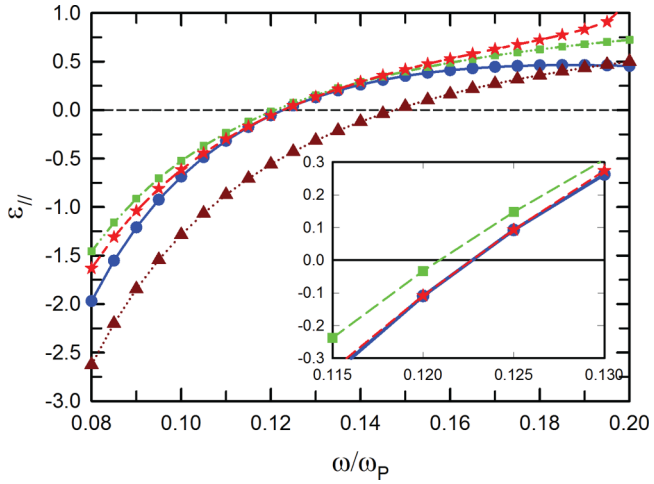

FIG. 1. Permittivity $\epsilon_{\|}$ vs normalized frequency ω/ω_p for a SL with small filling fraction $f = 1/21$ and width of the layers $a = \delta_0/2, b = 10\delta_0$. The red line (stars) is the exact result given by Eq. (18), the blue line (circles) is the effective permittivity obtained from Eq. (16), the green line (squares) plots Eq. (7), and the brown line (triangles) is the dependence obtained in the quasistatic limit (3). Insert shows a narrow region of frequencies near the point of topological transition $\omega/\omega_p = 0.123$.

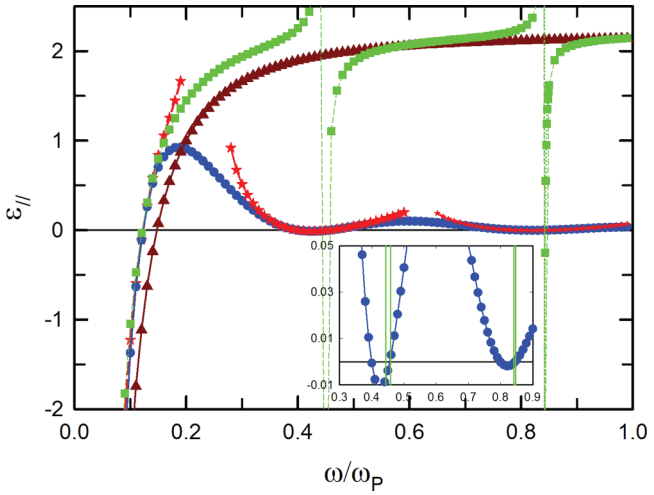

FIG. 2. The same as Fig. 1 but for a wider interval of frequencies.

approximation over the homogenization parameter $Kd \ll 1$. Nonlocal quadratic corrections can be calculated but they do not lead to new effects and can be neglected [21].

The exact result for $\epsilon_{\|}(\omega)$ is calculated directly from Eq. (13)

$$\epsilon_{||}(\omega) = \left(\frac{kc}{\omega}\right)^2 = \left[\frac{c}{d\omega}\arccos D_{\|}(\omega)\right]^2. \qquad (18)$$

This formula gives negative values for $\epsilon_{||}(\omega)$ since function $\arccos D_{\|}(\omega)$ is pure imaginary within the band gaps where $D(\omega) > 1$. The proposed dielectric function in Eq. (16) also becomes negative if $D(\omega) > 1$. For $D(\omega) < -1$ the function $\arccos D_{\|}(\omega)$ takes complex values, therefore the effective permittivity cannot be introduced using definition (18). The points where $D(\omega) = -1$ belong to the edge of the Brillouin zone, $Kd = \pi$, i.e., here the long-wavelength approximation is irrelevant. The method of homogenization valid at the edge of Brillouin zone was proposed in Ref. [24]. The same result (16) for the effective dielectric function can be obtained directly from Eq. (18) using the asymptotical expansion $\arccos x \approx \sqrt{2(1-x)}$, which is valid if $1 - x \ll 1$.

First we consider a SL with the parameters that were used in Refs. [7,10]. The thickness of the metal layer is $a = \delta_0/2$ and of the dielectric layer is $b = 10\delta_0$. The filling fraction of this SL is quite small, $f = a/(a+b) = 1/21$. The dielectric function of the metal is given by Drude model, $\epsilon(\omega) = 1 - \omega_p^2/\omega^2$ and for the dielectric $\epsilon_b = 2.25$. Figure 1 demonstrates the dependence $\epsilon_{\|}(\omega)$ obtained using Eqs. (3), (7), (16), and (18).

Looking at Fig. 1 one may conclude that for small filling fractions all three homogenization schemes represented by Eqs. (3), (7), and (16) give very similar results for $\epsilon_{||}(\omega)$. This impression, however, is due to the scale along the horizontal axis where frequency is measured in units of ω_p. Since for the noble metals $\omega_p \approx 9$ eV, even a small difference in the position of topological transition measured in ω/ω_p becomes quite large in the units of wavelength (nm). For small filling the topological transition occurs at relatively low frequencies where the error measured in the units of wavelength is emphasized by the small denominator in the formula $\Delta\lambda = -hc\Delta\omega/\omega^2$. Here $\Delta\omega$ is an error in the frequency (eV) and $\Delta\lambda$ is an error in the wavelength (cm). For example, the exact position of the topological transition in Fig. 1 is $\omega/\omega_p = 0.123$, which corresponds to the wavelength of 1120 nm. The point of transition obtained from Eq. (7) is red shifted by $0.002\omega/\omega_p$, that is, about 20 nm in the units of wavelength. The quasistatic approach Eq. (3) gives a blue shift by $0.024\omega/\omega_p$ for the transition frequency, that is, about 180 nm. If the error of 20 nm can be considered as acceptable for some optical measurement, then it is absolutely unacceptable if $\Delta\lambda = 180$ nm. Thus, the widely used quasistatic limit (3) gives too-large an error in the frequency of topological transition. Inapplicability of the quasistatic approach and Eq. (7) becomes more evident at higher frequencies. In Fig. 2 we plot the same functions as in Fig. 1 but for much wider interval of frequencies. The spectrum of the SL contains two more band gaps near the Γ point. They are quite narrow and the corresponding values of $\epsilon_{||}(\omega)$ are only slightly negative, as shown in the insert to Fig. 2. Within these bands the SL behaves as a metamaterial with epsilon near zero. Here a periodic layered structure may provide the bandwidth comparable with the bandwidth of the structures proposed in Ref. [42].

The approximation (16) is in excellent agreement with the exact result near every point of topological transition. Moreover, it can be used even away from these points. The only regions where this approximation fails are those where $D_{\|}(\omega) \leqslant -1$ and the dielectric function cannot be defined in a standard form of Eq. (18) because of complex values of $\arccos D_{\|}(\omega)$. Unlike this, the quasistatic approximation and Eq. (7) do not follow at all the behavior of the dielectric function at frequencies higher than the first topological transition at $\omega/\omega_p = 0.123$.

The situation with larger fillings also demonstrates that the validity of the homogenization approaches (3) and (7) may be questionable. When the metal filling increases the effective medium becomes more dispersive and the topological

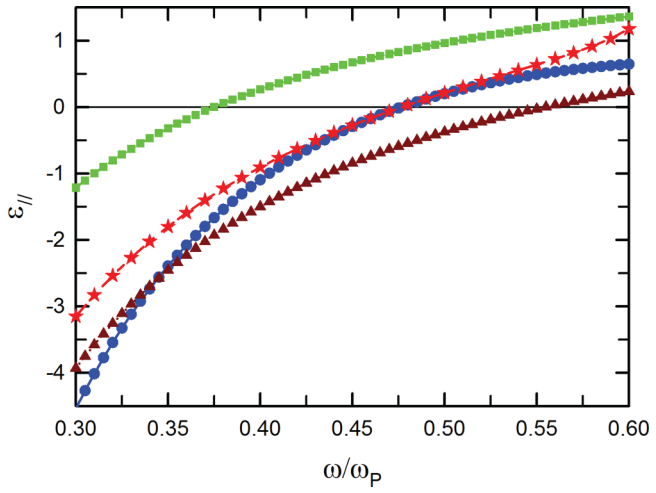

FIG. 3. The same as in Fig. 1 but for a SL with filling $f = 1/2$.

transition occurs at higher frequencies. Figure 3 shows the dispersion of the effective dielectric functions for a SL of the same constituents but with equal fillings, $a = b = 2\delta_0$. Since the thickness of the metal layer exceeds the skin depth, the electromagnetic field is strongly inhomogeneous inside it. The quasistatic approach completely ignores this fact, therefore it underestimates the value of the effective permittivity. The approach proposed in Ref. [10] takes into account the skin effect; however, the values of $\epsilon_{||}(\omega)$ obtained from Eq. (7) far exceed the exact result. Also this approach gives the position of the topological transition red shifted by 90 nm from the exact result of 290 nm (this wavelength corresponds to $\omega/\omega_p = 0.478$). The quasistatic approach gives too-small values for $\epsilon_{||}(\omega)$ and the frequency of the transition is blue shifted by 35 nm. Thus, the accuracy of both these approximations is not sufficient for modern optical studies. Unlike this, Eq. (16) exhibits frequency dispersion which is practically undistinguishable from the exact result within a wide interval of frequencies near the topological transition.

The accuracy of the quasistatic approach, which ignores spatial variations of the fields, becomes much better for a SL with narrower layers. Here the fields change smoothly and they can be approximated by constant (electrostatic) values. Since in a metal layer the fields oscillate at a shorter distance than in a dielectric, the width of the metal layer a should not exceed the skin depth δ_0 in order for the quasistatic approach to be valid.

Now we consider a SL which was fabricated to study an increase of radiative decay rate of rhodamine molecules placed in the vicinity of a hyperbolic metamaterial [43]. The SL consists of 16 alternating layers of gold and alumina. The thickness of each layer is $a = b = 19$ nm, i.e., for optical frequencies this is a deeply subwavelength region. The permittivity of alumina for optical frequencies is $\epsilon_b = 3.24$. The frequency dispersion for gold is taken in the following form:

$$\mathrm{Re}\,\epsilon(\omega) = 1 - \frac{\omega_p^2}{\omega^2 + \alpha^2\Gamma_p^2} + \frac{F_1\omega_1^2\left(\omega_1^2 - \omega^2\right)}{\left(\omega_1^2 - \omega^2\right)^2 + \Gamma_1^2\omega^2} + \frac{F_2\omega_2^2\left(\omega_2^2 - \omega^2\right)}{\left(\omega_2^2 - \omega^2\right)^2 + \Gamma_2^2\omega^2}, \tag{19}$$

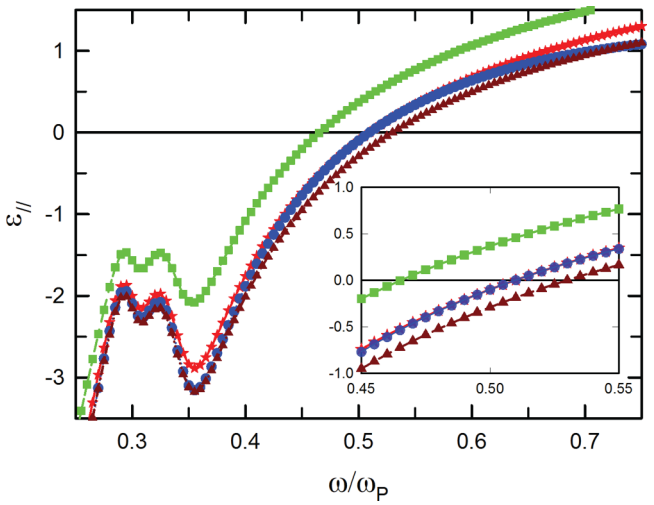

FIG. 4. Permittivity of a gold-alumina SL fabricated in Ref. [43]. The width of the layers is equal, $a = b = 19$ nm. The permittivity of the gold layer is modeled by Eq. (19) and the permittivity of alumina is $\epsilon_b = 3.24$. The labels for the curves are the same as in Fig. 1.

with Drude parameters from Johnson and Christy data [44] $\omega_p = 9$ eV and $\Gamma_p = 0.07$ eV, and with two Lorentzian oscillators with $F_1 = 0.3$, $\omega_1 = 2.7$ eV, $\Gamma_1 = 0.3$ eV, and $F_2 = 0.8$, $\omega_2 = 3.05$ eV, $\Gamma_2 = 0.5$ eV. The loss factor $\alpha = 1.35$ is introduced to modify the bulk value of gold damping term Γ_p. The optical skin depth for these metal parameters is $\delta_0 = c/\omega_p = 22$ nm, that is, slightly longer than the SL period. The rate of spontaneous emission near this hyperbolic metamaterial was evaluated by the authors of Ref. [43] using the quasistatic approach and a reasonable agreement with experimental data has been achieved. In order to evaluate the accuracy of the quasistatic approach we plot in Fig. 4 the dielectric function $\epsilon_{\|}(\omega)$ for this SL. The quasistatic approximation (dotted orange line) (3) turns out to be close to the exact result (red thick solid line) for all frequencies. It is seen in the insert to Fig. 4 that the position of the topological transition is blue shifted by 10 nm. Relatively good accuracy of the quasistatic approximation in this particular case is due to very narrow layer widths, which is less than the skin depth, and also due to high filling of metal that shifts the topological transition to ultraviolet region. Unlike this, the accuracy of Eq. (7) is reduced as compared to the case of small filling fractions. It gives an error of 30 nm in the position of the topological transition and the values of $\epsilon_{\|}(\omega)$ are considerably overestimated.

IV. PROPAGATION PARALLEL TO THE LAYERS

The Bloch vector for parallel propagation vanishes, $K_z = 0$. Let the wave propagates along the x axis with wave vector $k_x = k$. The dispersion equation (1) can be written as follows:

$$D_\perp(\omega,k) = \cosh[ap(\omega,k)]\cos[b\,q(\omega,k)] + \frac{1}{2}\left[\frac{|\epsilon(\omega)|q}{\epsilon_b p} - \frac{\epsilon_b p}{|\epsilon(\omega)|q}\right] \times \sinh[ap(\omega,k]\sin[b\,q(\omega,k] = 1. \tag{20}$$

Here

$$p(\omega,k)=\sqrt{k^2+\delta^{-2}(\omega)},\quad q(\omega,k)=\sqrt{(\omega/c)^2\epsilon_b-k^2}. \quad (21)$$

Unlike the dispersion equation (13) where frequency and wave vector are separated, these variables cannot be separated in general case in Eq. (20). The reason is lack of periodicity along the direction of propagation. One more principal physical difference between these two geometries is a possibility of propagation of surface plasmons along the layers. Depending on the sign of $q^2(\omega,q)$ the fields in the dielectric layer exhibit either oscillating

$$q^2=(\omega/c)^2\epsilon_b-k^2>0 \quad (22)$$

or evanescent

$$q^2=(\omega/c)^2\epsilon_b-k^2<0 \quad (23)$$

behavior along z. In the former case an eigenmode propagates due to partial reflection from the metal layers and partial penetration through them. In the latter case the trigonometric functions in Eq. (20) become evanescent, which is a signature of surface plasmon field in dielectric.

It is known that waveguide propagation is not allowed below some cut-off frequency ω_c. Unlike this, the spectrum of surface plasmon starts from zero frequency. Also the phase velocity of a waveguide mode (surface plasmon) is greater (less) than $c/\sqrt{\epsilon_b}$. These facts mean that the lowest allowed mode which propagates parallel to the layers is of plasmonic nature.

A. Plasmoniclike mode

It follows from Eq. (23) that the parameter $q(\omega,k)$ is pure imaginary, $q=iQ$. Having in mind the long-wavelength limit, we assume that

$$k\delta_0=\frac{kc}{\omega_p}\approx\frac{\omega\sqrt{\epsilon_b}}{\omega_p}\ll 1. \quad (24)$$

This inequality defines the frequencies where the conducting component of the SL exhibits metallic behavior. For typical metals this range extends up to near the UV region. Due to this inequality the k dependence in the parameter $p(\omega,k)$ can be neglected, i.e., $p\approx 1/\delta(\omega)$. Now the dispersion equation (20) is reduced to

$$\cosh\left[\frac{a}{\delta(\omega)}\right]\cosh(bQ)-\frac{1}{2}\left[\frac{|\epsilon(\omega)|Q\delta}{\epsilon_b}+\frac{\epsilon_b}{|\epsilon(\omega)|Q\delta}\right]\sinh\left[\frac{a}{\delta(\omega)}\right]\sinh(bQ)=1. \quad (25)$$

In the low-frequency limit the dispersion of surface plasmon is linear. Substituting the linear dependence $\omega=kc/\epsilon_\perp$ into Eq. (25) and expanding the hyperbolic functions in the limit $\omega,k\to 0$ the low-frequency effective dielectric constant of the SL is easily calculated,

$$\epsilon_\perp(\omega\to 0)=\epsilon_b\left[1+2\frac{\delta_0}{b}\tanh\left(\frac{a}{2\delta_0}\right)\right]. \quad (26)$$

This formula defines the slope of the plasmoniclike mode in the low-frequency limit. It is reduced to the well-known result $\epsilon_\perp=\epsilon_b$ if the neighboring unit cells are electromagnetically uncoupled, $\delta_0\ll a+b$. The static result (2), which for metal-dielectric SL is reduced to $\epsilon_\perp=\epsilon_b/(1-f)$, is obtained from Eq. (26) if the screening effect from the skin layer vanishes, i.e., $\delta_0\gg a$. Note that $\epsilon_\perp>\epsilon_b$, which means that in a multilayered metal-dielectric structure the plasmonic-like mode propagates slower than surface plasmon. This also becomes evident from Eq. (23), which is true only for the waves propagating slower than light.

B. Waveguidelike modes

At higher frequencies (and small k) the condition (22) becomes true and propagation of the modes with phase velocities greater than $c/\sqrt{\epsilon_b}$ is allowed. The spectrum consists of infinite number of waveguidelike modes. Each mode starts with finite cut-off frequency Ω_n at $k=0$ and at $k\to\infty$ it approaches the light line. The series of cut-off frequencies, $\omega=\Omega_n$, $n=1,2,\ldots$ are obtained from the equation

$$\cosh\left[\frac{a}{\delta(\omega)}\right]\cos\left(\frac{b\,\omega}{c}\sqrt{\epsilon_b}\right)+\frac{1}{2}\left[\sqrt{\frac{|\epsilon(\omega)|}{\epsilon_b}}-\sqrt{\frac{\epsilon_b}{|\epsilon(\omega)|}}\right]\sinh\left[\frac{a}{\delta(\omega)}\right]\sin\left(\frac{b\,\omega}{c}\sqrt{\epsilon_b}\right)=1. \quad (27)$$

The effective dielectric constant $\epsilon_\perp(\omega)$ must change its sign from negative to positive when frequency ω passes through any of the cut-off frequencies Ω_n. The asymptotical dependence $\epsilon_\perp(\omega)$ near Ω_n can be easily calculated from the exact dispersion equation (20). Explicit dispersion relation near the Γ point is obtained from Eq. (20) by expanding the function $D_\perp(\omega,k)$ at $k=0$ and $\omega=\Omega_n$,

$$D_\perp(\Omega_n,k=0)+\left[\frac{\partial D_\perp}{\partial\omega}+\frac{\partial D_\perp}{\partial q}\frac{\partial q}{\partial\omega}\right](\omega-\Omega_n)+\frac{\partial D_\perp}{\partial q}\frac{\partial q}{\partial k}k=1. \quad (28)$$

The derivatives in this equation are taken at $\omega=\Omega_n$ and $k=0$. According to Eq. (27) the first term equals 1. The derivatives $\partial q/\partial\omega=\sqrt{\epsilon_b}/c$ and $\partial q/\partial k=-kc/(\Omega_n\sqrt{\epsilon_b})$ are calculated from Eq. (22). Then the dispersion relation near a cut-off frequency turns out to be quadratic, i.e., $\omega-\Omega_n\propto k^2$. Similar quadratic dispersion is known from the theory of metallic waveguides. Quadratic dispersion relation gives rise to dielectric permittivity linearly vanishing near the cut-off frequency $\omega=\Omega_n$,

$$\epsilon_\perp(\omega)=\left(\frac{kc}{\Omega_n}\right)^2=\epsilon_b\left(1+\frac{c}{\sqrt{\epsilon_b}}\frac{\partial D_\perp/\partial\omega}{\partial D_\perp/\partial q}\right)\frac{\omega-\Omega_n}{\Omega_n}. \quad (29)$$

Here the derivatives of $D_\perp(\omega,q)$ can be easily calculated directly from Eq. (20),

$$\left.\frac{\partial D_\perp}{\partial\omega}\right|_{\substack{\omega=\Omega_n\\k=0}} = \frac{a}{c}\left[\sqrt{|\epsilon(\Omega_n)|}+\frac{\Omega_n}{2\sqrt{|\epsilon(\Omega_n)|}}\frac{d|\epsilon(\Omega_n)|}{d\Omega_n}\right]\left\{\sinh\left[\frac{a}{\delta(\Omega_n)}\right]\cos\left(\frac{b\,\Omega_n}{c}\sqrt{\epsilon_b}\right)+\frac{|\epsilon(\Omega_n)|-\epsilon_b}{2\sqrt{\epsilon_b|\epsilon(\Omega_n)|}}\right.$$
$$\left.\times\cosh\left[\frac{a}{\delta(\Omega_n)}\right]\sin\left(\frac{b\,\Omega_n}{c}\sqrt{\epsilon_b}\right)\right\}+\frac{|\epsilon(\Omega_n)|+\epsilon_b}{4\sqrt{\epsilon_b|\epsilon(\Omega_n)|}}\left[\frac{1}{|\epsilon(\Omega_n)|}\frac{d|\epsilon(\Omega_n)|}{d\Omega_n}-\frac{2}{\Omega_n}\right]\sinh\left[\frac{a}{\delta(\Omega_n)}\right]\sin\left(\frac{b\,\Omega_n}{c}\sqrt{\epsilon_b}\right), \tag{30}$$

$$\left.\frac{\partial D_\perp}{\partial q}\right|_{\substack{\omega=\Omega_n\\k=0}} = -b\cosh\left[\frac{a}{\delta(\Omega_n)}\right]\sin\left(\frac{b\,\Omega_n}{c}\sqrt{\epsilon_b}\right)+\delta(\Omega_n)\frac{|\epsilon(\Omega_n)|+\epsilon_b}{2\epsilon_b}\sinh\left[\frac{a}{\delta(\Omega_n)}\right]\sin\left(\frac{b\,\Omega_n}{c}\sqrt{\epsilon_b}\right)$$
$$+b\frac{|\epsilon(\Omega_n)|-\epsilon_b}{2\sqrt{\epsilon_b|\epsilon(\Omega_n)|}}\sinh\left[\frac{a}{\delta(\Omega_n)}\right]\cos\left(\frac{b\,\Omega_n}{c}\sqrt{\epsilon_b}\right). \tag{31}$$

While these formulas look quite cumbersome they serve to calculate only the numerical coefficient in the dispersion of the effective dielectric function (29).

C. Results and discussion

A typical band structure for propagation parallel to the layers is shown in Fig. 5. It is calculated from the dispersion relation (20) for a SL with low filling fraction $f = 1/21$. At low frequencies the spectrum starts from a plasmonic-like mode and above it there are several waveguidelike modes, depending on the number of real roots of Eq. (27) lying below ω_p [41]. The exact dispersion relations are shown by solid lines. The plots obtained in the effective medium approximation $\omega = kc/\sqrt{\epsilon_\perp(\omega)}$ are shown by dotted lines. The long-wavelength effective dielectric function $\epsilon_\perp$ is approximated by the constant value (26) for the plasmonic mode and by the linear function (29) for each of the waveguidelike modes. A piecewise continuous behavior of the effective dielectric function is shown in the right panel in Fig. 5. It can be seen that the proposed linear approximation gives the results which are very close to the exact ones. Moreover, the region where the effective medium approximation is valid turns out to be much wider than one may expect from the long-wavelength limit $kd \ll 1$.

For the SL with small filling, $f = 1/21$, the plasmonic mode exhibits linear dispersion up to $kd \approx 3$. The slope of this mode is indistinguishable from that given by Eq. (26)

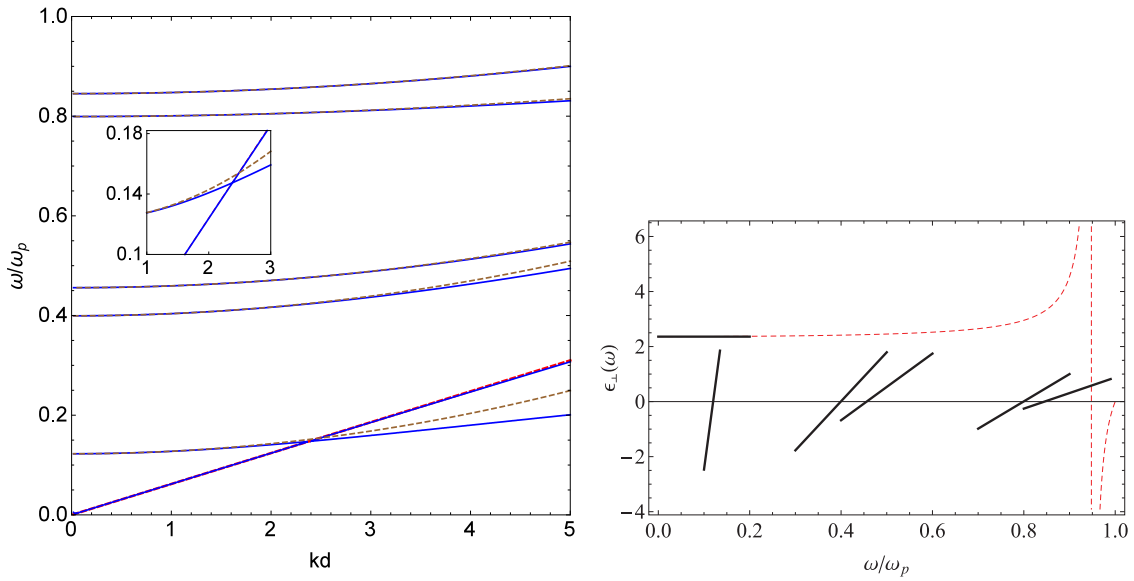

FIG. 5. Propagation parallel to the layers in a SL with low filling, $f = 1/21$. Left panel: Band structure (blue solid lines) calculated from the exact equation (20). It consists of a single plasmonic mode which starts at $\omega = 0$ and five waveguidelike modes starting at cut-off frequencies Ω_n calculated from Eq. (27). The results of the effective medium approximation $\omega = kc/\sqrt{\epsilon_\perp(\omega)}$ with $\epsilon_\perp(\omega)$ given by Eq. (29) are shown by dashed orange lines. The dispersion of the plasmonic mode is almost linear; therefore the exact curve practically coincides with the straight line of the effective medium approximation shown by dashed red line. For all the waveguidelike modes the proposed parabolic approximation are in excellent agreement with the exact results. Insert: Blowup of the region of crossing of the plasmonic mode and the lowest waveguidelike mode. Even on this scale the exact and approximate lines for the plasmonic mode are undistinguishable. Right panel: Effective dielectric function vs frequency (solid lines). For the plasmonic mode the effective dielectric function (26) is frequency independent. Near each cut-off frequency Ω_n the effective dielectric function $\epsilon_\perp(\omega)$ exhibits linear behavior with different slopes. The quasistatic approximation (2) is shown by the dashed red line.

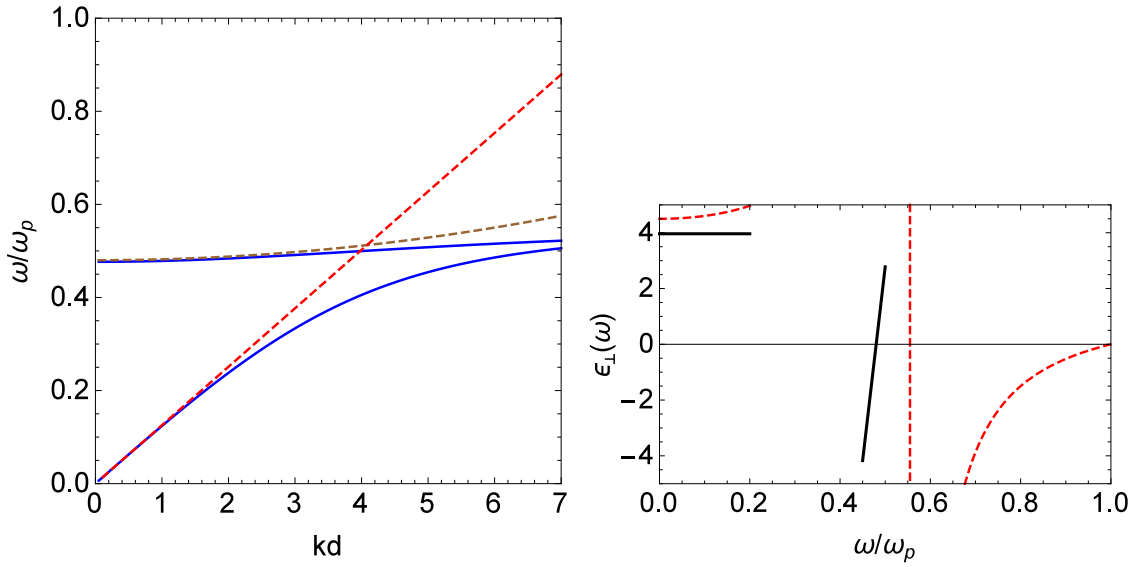

FIG. 6. Propagation parallel to the layers for a SL with high filling, $f = 1/2$ and $a = b = 2\delta$. Left panel: Band structure (blue solid lines) calculated from the exact equation (20). It consists the plasmonic mode which starts at $\omega = 0$ and of single waveguidelike mode starting at cut-off frequency $\Omega_1 = 0.48$ calculated from Eq. (27). The result of the effective medium approximation $\omega = kc/\sqrt{\epsilon_\perp(\omega)}$ with $\epsilon_\perp(\omega)$ given by Eq. (29) is shown by dashed orange line. Unlike the plasmonic mode in Fig. 5, here the dispersion of the plasmonic mode is strongly nonlinear. Therefore, the effective medium approximation (straight red dashed line) is close to the exact curve only for $kd < 2$, which is still wider that is expected for the long-wavelength limit. For the waveguidelike mode the proposed parabolic approximation are in excellent agreement with the exact results for $kd < 3$. Right panel: Effective dielectric function vs frequency (black solid lines). For the plasmonic mode the effective dielectric function (26) is frequency independent, $\epsilon_\perp = 3.96$. Near the cut-off frequency Ω_1 the effective dielectric function $\epsilon_\perp(\omega)$ exhibits linear behavior. The quasistatic approximation (2) is plot by dashed red line. It shows quite different results within the whole range of frequencies.

(shown by dashed red line). Due to very low filling, the slope of the plasmonic mode is practically the same as that for the light line $\omega/k = \sqrt{\epsilon_b}$. This occurs because the correction to $\epsilon_b = 2.25$ given by Eq. (26) in this case is small, $2(\delta_0/b)\tanh(a/2\delta_0) \approx 0.11$. Sublinear dispersion of the plasmonic mode can be seen for much larger values of the wave vector, at $kd > 10$. The dispersion of the waveguidelike modes is very well approximated by the proposed parabolic dependence Eq. (29). There are five waveguidelike modes with cut-off frequencies $\Omega_1 = 0.12\omega_p$, $\Omega_2 = 0.399\omega_p$, $\Omega_3 = 0.456\omega_p$, $\Omega_4 = 0.799\omega_p$, and $\Omega_5 = 0.845\omega_p$. For the lowest band the parabolic approximation is valid up to $kd \approx 3$, i.e., the region of validity is the same as that for the plasmonic mode. The dispersion curves for these two modes cross at $kd \approx 2.7$. This region is shown in the insert. For the higher waveguidelike modes the region of validity of parabolic approximation is even wider. It extends up to $kd = 4$ for the second mode, to $kd = 5$ for the third and forth modes, and to $kd = 7$ for the highest, fifth, mode.

The graph for the effective dielectric function $\epsilon_\perp(\omega)$ consists of several straight lines with different slopes, shown in Fig. 5 (right panel). In the region of low frequencies only the plasmonic mode exists for which $\epsilon_\perp(\omega)$ is a positive constant given by Eq. (26). Passing through any of the cut-off frequencies Ω_n the effective dielectric function $\epsilon_\perp(\omega)$ changes its sign. All the transitions occur linearly. However, the rates of the transitions differ. The fastest transition takes place near Ω_1 where $\epsilon_\perp(\omega) = 123.5(\omega/\omega_p - 0.12)$. For higher modes the rate of transition gradually decreases. The slowest transition occurs for the fifth mode where $\epsilon_\perp(\omega) = 5.66(\omega/\omega_p - 0.845)$, i.e., the rate is decreased by 20 times. The dashed red line in Fig. 5 shows the dispersion of the effective permittivity obtained from the quasistatic limit (2). It is clear that the quasistatic approximation is valid only at low frequencies where the plasmonic mode exists. Because of the very low filling fraction the effective dielectric constant for plasmonic mode is close to ϵ_b. In this case Eqs. (2) and (26) give the values close to ϵ_b. However, for higher frequencies the quasistatic approximation is not valid at all. It predicts sign change at $\omega = 0.95\omega_p$, which is not close to any of the cut-off frequencies obtained from the exact equation (27). Thus, in a SL with a low filling fraction the quasistatic approximation is not valid above the first cut-off frequency. In Fig. 6 we plot the band structure and the results of the effective medium theory for a SL with $f = 1/2$ and $a = b = 2\delta_0$. Here the eigenfrequency of the plasmonic mode has a clear tendency to saturation if $kd > 7$. For $kd < 32$ the dispersion is close to linear with the slope given by Eq. (26). In this case the effective dielectric constant $\epsilon_\perp = 2.25(1 + \tanh 1) \approx 3.96$ is greater than $\epsilon_b = 2.25$; therefore the plasmonic mode in this SL propagates essentially slower than surface plasmon along a metal-dielectric boundary with the same dielectric parameters. Due to the higher filling fraction this SL exhibits much stronger "metallic" behavior than the previous one with $f = 1/21$. In particular, there is only a single waveguidelike mode with cut-off frequency at $\Omega_1 = 0.48$. The dispersion of this mode is well approximated (for $kd < 3$) by a parabola $\omega/\omega_p - 0.48 = 1.95 \times 10^{-3}(kd)^2$, shown in Fig. 6 by dashed orange line. The corresponding effective dielectric function is approximated by a linear dependence $\epsilon_\perp(\omega) = 139(\omega/\omega_p - 0.48)$. It is

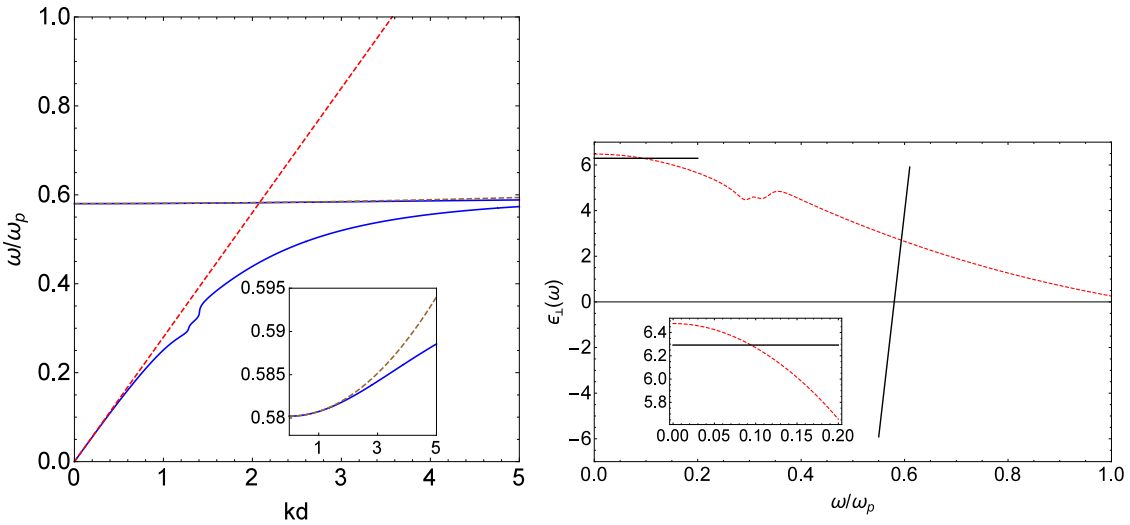

FIG. 7. Propagation parallel to the layers for gold-alumina SL fabricated in Ref. [43]. The layers are of equal width, $a = b = 19$ nm. The permittivity of gold layer is modeled by Eq. (19) and the permittivity of alumina is $\epsilon_b = 3.24$. Left panel: Band structure (blue solid lines) calculated from the exact equation (20). It consists of the plasmonic mode, which starts at $\omega = 0$, and of the waveguidelike mode starting at cut-off frequency $\Omega_1 = 0.58$ calculated from Eq. (27). The result of the effective medium approximation $\omega = kc/\sqrt{\epsilon_\perp(\omega)}$ with $\epsilon_\perp(\omega)$ calculated from Eq. (29) is shown by a dashed orange line. Unlike the plasmonic mode in Fig. 5, here the dispersion of the plasmonic mode is strongly nonlinear. Therefore, the effective medium approximation (straight red dashed line) is close to the exact curve only for $kd < 1$. The waveguidelike mode exhibits very weak dependence on the parameter kd. In accordance with this, the proposed parabolic approximation has very small curvature and it is in excellent agreement with the exact results for $kd < 4$. The insert shows blowup of the flat waveguidelike band. Right panel: Effective dielectric function vs frequency (black solid lines). For the plasmonic mode the effective dielectric function (26) is frequency independent, $\epsilon_\perp = 6.29$. Near the cut-off frequency Ω_1 the effective dielectric function $\epsilon_\perp(\omega)$ exhibits sharp topological transition. The quasistatic approximation (2) is plotted with dashed red line. It is valid at low frequencies only. This region is shown in the insert.

shown by a black solid line (right panel of Fig. 6). For this SL the quasistatic approximation (dashed red line) does not give satisfactory results. Even at very low frequencies it gives $\epsilon_\perp = 4.5$, which exceeds the result of the effective medium approximation $\epsilon_\perp = 3.96$. For higher frequencies the discrepancy is even bigger.

Numerical results for the gold-alumina SL [43] are plotted in Fig. 7. Like in the previous case with the same filling fraction $f = 1/2$, the spectrum contains only a single waveguidelike mode. It starts at the cut-off frequency $\Omega_1 = 0.58$ and exhibits very weak dependence on the wave vector k. This dependence is given by the parabola $\omega/\omega_p = 0.58 + 5.5 \times 10^{-3}(kd)^2$. Due to very small curvature this parabola can be approximately considered as an example of a flat band. Periodic systems with macroscopically degenerated flat bands attract a lot of attention. Due to the dispersionless character of the corresponding mode, the Bloch functions are represented by strongly localized states. It was shown that the basis formed by localized states may lead to the existence of new topological phases and an anomalous Anderson transition, the appearance of Fano resonances, and many other interesting effects [45–50]. While the band in Fig. 7 is not exactly flat—weak dependence on kd is seen in the insert—the gold-alumina SL may be considered as a good approximation of a real system with approximately flat band. Because of flatness of the waveguidelike band the topological transition at Ω_1 is very sharp; see the black solid line in the right panel of Fig. 7. It is described by a linear dependence $\epsilon_\perp(\omega) = 197(\omega/\omega_p - 0.58)$. The rate of this transition is the highest among the others that we consider. For a perfectly flat band the rate becomes infinite, i.e., the transition occurs along a vertical line.

The quasistatic approximation Eq. (2) for gold-alumina SL can be used only at low frequencies where plasmonic mode exhibits linear dispersion. Even here it gives an error of ∼5%; see the insert to Fig. 7, right panel. For higher frequencies the static approximation becomes invalid. In the experiment [43] the measurements were performed at the wavelengths exceeding 630 nm. This region corresponds to the interval $\omega/\omega_p < 0.2$ in Fig. 7, where the quasistatic approximation is still valid; therefore the authors of Ref. [43] reported a good agreement between their experimental results and theoretical predictions made on the basis of the quasistatic approximation.

Since the proposed approach for calculation of the effective dielectric tensor of a layered medium is valid not only near the frequencies of topological transitions but also within a wide range of frequencies where the dielectric function is not close to zero, it can be used for engineering layered samples with dielectric constants matching some prescribed values. Such a sample may exhibit anomalously weak scattering of electromagnetic waves if its dielectric constants match those of the environment [51].

V. CONCLUSIONS

In conclusion, we have proposed an analytical approach for calculation of the effective dielectric functions $\epsilon_\parallel(\omega)$ and $\epsilon_\perp(\omega)$ of metal-dielectric superlattices which gives asymptotically correct results in the long-wavelength limit. It gives the exact

positions for all frequencies of the topological transitions where one of the dielectric functions changes its sign. Near any of the frequencies of the topological transition the accuracy of the proposed theory exceeds that of any other known approaches. In particular, it is shown that the widely used formulas Eqs. (2) and (3) obtained by Rytov [6] in the quasistatic approach may be not applicable at all, or their accuracy turns out to be insufficient for modern optical studies. The accuracy of the quasistatic approach becomes low if the width of the metallic layer exceeds the skin depth. Applications of hyperbolic metamaterials are due to their ability to increase the rate of spontaneous emission. The rate increase depends on the both components of the dielectric tensor [52] and if even one of these components gives a considerable error as a result of quasistatic approximation, the frequency dependence of the rate of spontaneous emission may be incorrect, as shown in Ref. [15,16]. This is of particular importance for the type 1 hyperbolic metamaterials when the component $\epsilon_{\perp}(\omega)$ changes its sign, since the quasistatic approach is not applicable near the frequency where $\epsilon_{\perp}(\omega) = 0$.

ACKNOWLEDGMENT

V.P.D. thanks the Army Research Office for support, Grant No. W911NF-11-1-0333, and J.A. thanks CONACyT, Mexico, Grant No. 167939, for support.

[1] D. R. Smith and D. Schurig, Phys. Rev. Lett. **90**, 077405 (2003); D. R. Smith, D. Schurig, J. J. Mock, P. Kolinko, and P. Rye, Appl. Phys. Lett. **84**, 2244 (2004).
[2] M. A. Noginov, Yu. A. Barnakov, G. Zhu, T. Tumkur, H. Li, and E. E. Narimanov, Appl. Phys. Lett. **94**, 151105 (2009).
[3] V. P. Drachev, V. A. Podolskiy, and A. V. Kildishev, Opt. Express **21**, 15048 (2013).
[4] A. Poddubny, I. Iorsh, P. Belov, and Yu. Kivshar, Nat. Photon. **7**, 948 (2013).
[5] M. A. Noginov, H. Li, Y. A. Barnakov, D. Dryden, G. Nataraj, G. Zhu, C. E. Bonner, M. Mayy, Z. Jacob, and E. E. Narimanov, Opt. Lett. **35**, 1863 (2010); A. N. Poddubny, P. A. Belov, P. Ginzburg, A. V. Zayats, and Yu. S. Kivshar, Phys. Rev. B **86**, 035148 (2012); W. D. Newman, C. L. Cortes, and Z. Jacob, J. Opt. Soc. Am. B **30**, 766 (2013); Lei Gu, J. E. Livenere, G. Zhu, T. U. Tumkur, H. Hu, C. L. Cortes, Z. Jacob, S. M. Prokes, and M. A. Noginov, Sci. Rep. **4**, 7327 (2014); T. Galfsky, H. N. S. Krishnamoorthy, W. Newman, E. E. Narimanov, Z. Jacob, and V. M. Menon, Optica **2**, 63 (2015).
[6] S. M. Rytov, Zh. Eksp. Teor. Fiz. **29**, 605 (1956) [Sov. Phys. JETP **2**, 466 (1956)].
[7] X. Xu, Y. Xi, D. Han, X. Liu, J. Zi, and Z. Zhu, Appl. Phys. Lett. **86**, 091112 (2005).
[8] J. B. Pendry, A. J. Holden, W. J. Stewart, and I. Youngs, Phys. Rev. Lett. **76**, 4773 (1996).
[9] M. G. Silveirinha, Phys. Rev. E **73**, 046612 (2006).
[10] B. Zenteno-Mateo, V. Cerdán-Ramírez, B. Flores-Desirena, M. P. Sampedro, E. Juárez-Ruiz, and F. Pérez-Rodríguez, Progr. Electromagnet. Res. Lett. **22**, 165 (2011).
[11] V. Cerdán-Ramírez, B. Zenteno-Mateo, M. P. Sampedro, M. A. Palomino-Ovando, B. Flores-Desirena, and F. Pérez-Rodríguez, J. Appl. Phys. **106**, 103520 (2009); J. A. Reyes-Avendaño, U. Algredo-Badillo, P. Halevi, and F. Pérez-Rodríguez, New J. Phys. **13**, 073041 (2011).
[12] D. Stroud and F. P. Pan, Phys. Rev. B **17**, 1602 (1978).
[13] H. Herzig Sheinfux, I. Kaminer, Y. Plotnik, G. Bartal, and M. Segev, Phys. Rev. Lett. **113**, 243901 (2014).
[14] A. Andryieuski, A. V. Lavrinenko, and S. V. Zhukovsky, Nanotechnology **26**, 184001 (2015); S. V. Zhukovsky, A. Andryieuski, O. Takayama, E. Shkondin, R. Malureanu, F. Jensen, and A. V. Lavrinenko, Phys. Rev. Lett. **115**, 177402 (2015).
[15] O. Kidwai, S. V. Zhukovsky, and J. E. Sipe, Opt. Lett. **36**, 2530 (2011).
[16] O. Kidwai, S. V. Zhukovsky, and J. E. Sipe, Phys. Rev. A **85**, 053842 (2012).
[17] R. C. McPhedran, L. C. Botten, M. S. Craig, M. Nevière, and D. Maystre, Opt. Acta: Int. J. Opt. **29**, 289 (1982).
[18] J. Elser, V. A. Podolskiy, I. Salakhutdinov, and I. Avrutsky, Appl. Phys. Lett. **90**, 191109 (2007).
[19] A. V. Chebykin, A. A. Orlov, C. R. Simovski, Yu. S. Kivshar, and P. A. Belov, Phys. Rev. B **86**, 115420 (2012).
[20] Ruey-Lin Chern, Opt. Express **21**, 16514 (2013).
[21] Alessandro. Ciattoni and Carlo. Rizza, Phys. Rev. B **91**, 184207 (2015).
[22] L. D. Landau, E. M. Lifshitz, and L. P. Pitaevskii, *Electrodynamics of Continuous Media*, 2nd ed. (Pergamon, Oxford, 1984).
[23] Igor I. Smolyaninov, Phys. Rev. D **85**, 114013 (2012).
[24] R. V. Craster, J. Kaplunov, and A. V. Pichugin, Proc. R. Soc. A **466**, 2341 (2010).
[25] J. B. Keller, J. Math. Phys. **5**, 548 (1964).
[26] W. I. Perrins, D. R. McKenzie, and R. C. McPhedran, Proc. R. Soc. Lond. A **369**, 207 (1979).
[27] D. J. Bergman and K. J. Dunn, Phys. Rev. B **45**, 13262 (1992).
[28] P. Lalanne, Phys. Rev. B **58**, 9801 (1998).
[29] P. Halevi, A. A. Krokhin, and J. Arriaga, Phys. Rev. Lett. **82**, 719 (1999).
[30] A. A. Krokhin and E. Reyes, Phys. Rev. Lett. **93**, 023904 (2004).
[31] Yu. A. Godin, J. Math. Phys. **54**, 053505 (2013).
[32] M. G. Silveirinha, J. D. Baena, L. Jelinek, and R. Marques, Metamaterials **3**, 115 (2009).
[33] G. P. Ortiz, B. E. Martínez-Zérega, B. S. Mendoza, and W. L. Mochán, Phys. Rev. B **79**, 245132 (2009).
[34] C. Fietz and G. Shvets, Physica B **405**, 2930 (2010); Phys. Rev. B **82**, 205128 (2010).
[35] C. R. Simovski, J. Opt. **13**, 013001 (2011).
[36] A. P. Vinogradov, A. I. Ignatov, A. M. Merzlikin, S. A. Tretyakov, and C. R. Simovski, Opt. Express **19**, 6699 (2011).
[37] Andrea Alù, Phys. Rev. B **84**, 075153 (2011).
[38] A. Pors, I. Tsukerman, and S. I. Bozhevolnyi, Phys. Rev. E **84**, 016609 (2011).
[39] I. Tsukerman and V. A. Markel, Proc. R. Soc. A **470**, 20140245 (2014).
[40] H. N. S. Krishnamoorthy, Z. Jacob, E. Narimanov, I. Kretzschmar, and V. M. Menon, Science **336**, 205 (2012).

[41] P. Markoš and C. M. Soukoulis, *Wave Propagation. From Electrons to Photonic Crystals and Left-Handed Materials* (Princeton University Press, Princeton, NJ, 2008).
[42] A. V. Goncharenko, V. U. Nazarov, and K.-R. Chen, Opt. Mater. Express **3**, 143 (2013).
[43] J. Kim, V. P. Drachev, Z. Jacob, G. V. Naik, A. Boltasseva, E. E. Narimanov, and V. M. Shalaev, Opt. Express **20**, 8100 (2012).
[44] P. B. Johnson and R. W. Christy, Phys. Rev. B **6**, 4370 (1972).
[45] D. N. Christodoulides, F. Lederer, and Y. Silberberg, Nature **424**, 817 (2003).
[46] M. Goda, S. Nishino, and H. Matsuda, Phys. Rev. Lett. **96**, 126401 (2006).
[47] A. E. Miroshnichenko, S. Flach, and Yu. S. Kivshar, Rev. Mod. Phys. **82**, 2257 (2010).
[48] E. J. Bergholtz and Z. Lu, Int. J. Mod. Phys. B **27**, 1330017 (2013).
[49] S. Flach, D. Leykam, J. D. Bodyfelt, P. Matthies, and A. S. Desyatnikov, Europhys. Lett. **105**, 30001 (2014); **106**, 19901 (2014).
[50] J. D. Bodyfelt, D. Leykam, C. Danieli, X. Yu, and S. Flach, Phys. Rev. Lett. **113**, 236403 (2014).
[51] H. Shen, D. Lu, B. VanSaders, J. J. Kan, H. Xu, E. E. Fullerton, and Zh. Liu, Phys. Rev. X **5**, 021021 (2015).
[52] Z. Jacob, J. Y. Kim, G. V. Naik, A. Boltasseva, E. E. Narimanov, and V. M. Shalaev, Appl. Phys. B **100**, 215 (2010).